Korean J. Chem. Eng., **27**(1), 116-120 (2010)
DOI: 10.1007/s11814-009-0313-5

Removal of the antibiotic tetracycline by Fe-impregnated SBA-15

Bao Khanh Vu*, Eun Woo Shin*,†, Olga Snisarenko*, Wang Seok Jeong, and Hak Sung Lee***

*School of Chemical Engineering and Bioengineering, University of Ulsan,
Daehakro 102, Nam-gu, Ulsan 680-749, Korea
**Taewha Environment Co. Ltd., 34-1 Seonam-dong, Nam-gu, Ulsan, Korea
(*Received 28 October 2008 • accepted 23 June 2009*)

Abstract−We prepared Fe-impregnated mesoporous silicates to investigate the adsorption of tetracycline in aqueous solution. Mesoporous silicates with different Fe content (5, 10, 30, 50 wt%) were prepared by an incipient wetness method. Adsorption kinetics for tetracycline showed that Fe-impregnation improved the adsorption ability for tetracycline. By fitting the adsorption kinetic data to a pseudo second-order model, we obtained a maximum adsorption amount of tetracycline with Fe_{30}SBA-15 (30 wt% Fe-impregnated mesoporous silicates) at 41.7 mg/g. The pH dependency of tetracycline adsorption exhibited a volcano curve where the maximum adsorption onto the Fe_{30}SBA-15 sample occurred in the neutral pH region. The introduction of Fe species into the SBA-15 revived the adsorption ability for tetracycline, whereas there was no interaction between tetracycline and SBA-15, a mesoporous silicate. These results suggest that impregnated Fe species produce an effective interaction with tetracycline in an aqueous system.

Key words: Tetracycline, Fe-impregnation, Mesoporous Silicates, Adsorption

INTRODUCTION

Pollution of water bodies by antibiotics has become a concern due to the extensive use of antibiotics in human infection and veterinary medicine worldwide and their poor absorption by the human and animal body after intake [2]. They have been detected in surface water, groundwater, and wastewater [1]. Because of the dispersion of manure and sewage sludge in fields as fertilizers, antibiotics have the potential to reach aquatic environments [3-6].

Tetracycline is a well known antibiotic characterized by multiple ionizable functional groups that exist predominantly as zwitterions at neutral pH values (Fig. 1). Tetracycline contains three functional groups: tricarbonylamide (C-1:C-2:C-3), phenolic diketone (C-10:C- 11:C-12), and dimethylamine (C-4); each functional group has a different pKa (3.3, 7.68 and 9.69, respectively) [7]. The characteristics of tetracycline confer a marked pH-dependent behavior on solubility and lipophilicity so that it exists as a cationic, zwitterionic, or anionic species under acidic, moderately acidic to neutral, and alkaline conditions, respectively. The ionization behavior can significantly influence tetracycline sorption; at pH 7, tetracycline species are 84% zwitterionic and 16% anionic [8].

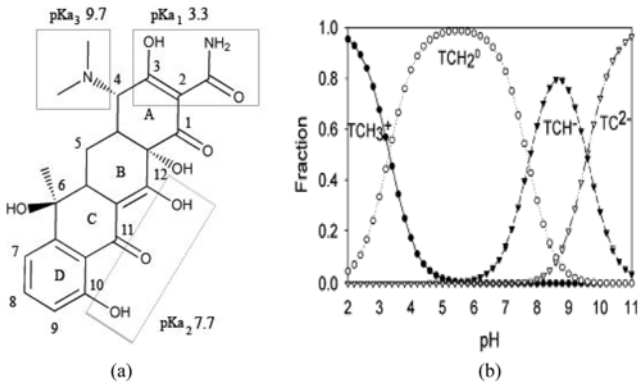

Fig. 1. (a) Structure of tetracycline and (b) pH-dependent speciation of tetracycline.

Because the maximum permissible concentration (MPC) of tetracycline in aqueous solutions for industrial and pharmacy wastewaters is very low (0.001 mg/L), one of the most efficient and promising methods for removing it is the adsorption process [9,10]. Achieving an MPC for tetracycline (0.001 mg/L) in aqueous solutions through the adsorption process requires an adsorbent with a high sorption capacity and high selectivity. Surface-functionalized mesoporous materials have recently been intensively studied as adsorbents due to their large surface area, fast adsorption kinetics, controllable pore size, and regular pore arrangement [11-13]. Mesoporous and nonporous SiO_2 and Al_2O_3 adsorbents were used as adsorbents for antibiotic ofloxacin, displaying a 1.5 μmol m^{-2} adsorption capacity for this antibiotic [14]. To improve adsorption capacity, several mesoporous silicates have been functionalized with different ligands and active components depending on the toxic heavy metals traces [12,15-18] and various organic components in the contaminated waters [19,20].

Fe species are widely used as active components for removing pollutants from water [21,22]. According to previous reports, Fe-impregnation into parent materials such as lignocellulosic materials considerably enhances their adsorption capacity [22]. In this study, Fe-impregnated mesoporous silicates were applied to the adsorption of tetracycline. SBA-15 was prepared as a parent silicate and impregnated with Fe species by an incipient wetness impregnation technique. The characteristics of the prepared materials were examined by N_2 gas isotherm analysis and FTIR, and the interaction of

†To whom correspondence should be addressed.
E-mail: ewshin@mail.ulsan.ac.kr

tetracycline with the prepared materials in aqueous solution was investigated by studying adsorption kinetics and envelopes.

EXPERIMENTAL

1. Materials

SBA-15 was synthesized using triblock copolymer (Pluronic P123, $EO_{20}PO_{70}EO_{20}$) as a structure-directing reagent and tetraethyl orthosilicate (TEOS) as a silica precursor. Four grams of triblock copolymer was dissolved in 60 ml of deionized water for 30 min, and 120 ml of 2 M hydrochloric acid solution was added. The mixed solution was stirred for 30 min. Tetraethyl orthosilicate was then added to the mixture and heated at 35 °C for 20 h. The mixture was transferred into a Teflon bottle and heated at 90 °C for 24 h without stirring. The solid product was then filtered using 0.45 μm filter papers and dried at room temperature under a vacuum before calcination. The mole fraction of each component for as-synthesized SBA-15 was 1 mol TEOS: 5.85 mol HCl: 163 mol H_2O: 0.0168 mol triblock copolymer. Calcination was performed in an oven at 550 °C for 6 h with air to remove the triblock copolymer organic component. The calcined SBA-15 was preserved at room temperature under a vacuum. All the chemicals used in this study were purchased from Sigma-Aldrich (USA).

Fe species were impregnated into SBA-15 with different loading amounts (5, 10, 30, and 50 wt%). The percentage of Fe impregnation onto SBA-15 in this study can be explained by the following equation:

$$\text{Fe impregnated (\%)} = \frac{\text{Mass of Fe added to SBA}-15}{\text{Mass of SBA}-15} \cdot 100\% \quad (1)$$

Fe-impregnation was conducted by the incipient wetness impregnation technique, and $Fe(NO_3)_3 \cdot 9H_2O$ was used as the iron precursor for incorporation into the SBA-15. An aliquot of 200-μL iron precursor solution was evenly dispersed by using a 200-μL syringe over 1 gram of calcined SBA-15 placed into a mortar. The mixture was homogeneously mixed in the mortar with a pestle for approximately 5 minutes. The procedure of adding 200-μL of the metal precursors solution to the mortar was repeated until the ratio of the metal precursor solution volume (mL) and SBA-15 mass (g) was 2 : 1. The final mixture was then dried under a vacuum hood at room temperature for 1 day. The solid was calcined in a furnace with a programmed temperature increase from room temperature to 550 °C with a ramping speed of 0.5 °C min-1. The prepared Fe-impregnated SBA-15 was designated as Fe_xSBA-15, where x denotes the weight percent of Fe in the sample.

2. Adsorption Tests

To investigate the adsorption behavior towards tetracycline, kinetic studies were conducted with mesoporous adsorbents at pH 7 and an initial tetracycline solution concentration of 100 mg/L. A 3.5 mL aliquot of tetracycline stock solution and 30 mL of deionized water, each buffered at the appropriate ionic strength, were added to 500 mL flasks and wrapped by aluminum foil to protect the solution from sunlight [23-25]. Thirty milligrams of Fe_xSBA-15 was added to the solution and the solution pH was maintained at 7 using 0.1 M HCl and 0.1 M NaOH as a titrant with manual checks every 30 min during all periods of the tetracycline adsorption test. A magnetic stirrer was used to ensure compounds were completely dissolved. Two milliliters of suspension was sampled with a syringe after 0.25, 0.5, 1, 2, 4, 8, 12, 24, 28, and 36 hours of reaction. The sampled suspension was immediately filtered with a membrane filter (0.45 μm nominal pore size), and the filtrate was stored at 5 °C until analyzed. A pseudo second-order kinetic equation was found to fit well for many of the chemisorption processes using heterogeneous materials [26]. All of the kinetic data from our experiments were well fitted with a pseudo second-order kinetic model when estimating the rate constants and adsorption capacities of tetracycline. The pseudo second-order kinetic equation is as follows:

$$\frac{dq_t}{dt} = k(q_e - q_t)^2 \quad (2)$$

where k is second-order sorption equilibrium rate constant (g/mg·min) and q_t is the amount adsorbed at time t (mg/g).

Adsorption envelopes were obtained for tetracycline at an initial solution concentration of 100 mg/L. The stock solution of tetracycline (tetracycline hydrochloride - Sigma-Aldrich, assay ≥96.0%) was prepared at a tetracycline concentration of 1,000 mg/L. A given amount of 0.1 M HCl or 0.1 M NaOH was added to the solution to obtain a final supernatant pH value in the range of 3-10. All eight flasks were stirred by an agitation shaker for 24 hour. After equilibration, the pH of the supernatant was measured, and the supernatant was passed through a membrane filter (0.45 μm nominal pore size) and stored at 5 °C until analyzed.

3. Characterization

After preparation, the physicochemical characteristics of all materials were evaluated by using nitrogen adsorption/desorption isotherms and Fourier transform infrared (FTIR) spectroscopy. The infrared spectra of the samples in the form of KBr powder-pressed pellets were measured on a Nicolet 380 FT-IR spectrophotometer (USA) under ambient conditions. A Micromeritics ASAP 2020 (USA) (a surface area and pore size analyzer) was used to determine the nitrogen sorption characteristics of the samples. The surface area was calculated by the conventional BET method. The Barett, Joyner and Halenda (BJH) method was used to calculate pore parameters from the adsorption branches of these isotherms.

RESULTS AND DISCUSSION

1. Characterization of Materials

Nitrogen adsorption/desorption isotherms of all the samples are represented in Fig. 2. All the patterns show typical irreversible type IV isotherms with an H1 hysteresis loop as defined by the International Union of Pure and Applied Chemistry (IUPAC) [27]. In the isotherms of SBA-15, the volumes adsorbed inflected sharply in the range between 0.6 and 0.7 of relative pressure (P/P_0). The sharpness of these steps indicated that the mesopores of those samples were uniform [28]. In contrast, for Fe-impregnated SBA-15, shoulders were observed in the desorption branch of the hysteresis loop, indicating that those samples had mesopores of two different sizes, affected by Fe-impregnation. In addition, the sharpness of the inflection step gradually decreased with Fe-impregnations at the same position.

The calculated BET surface areas and the average pore sizes based on the Barrett, Joyner, and Halenda (BJH) analysis are shown in Table 1. BET surface areas (A_{BET}) decreased from 751 to 348.7 m^2/

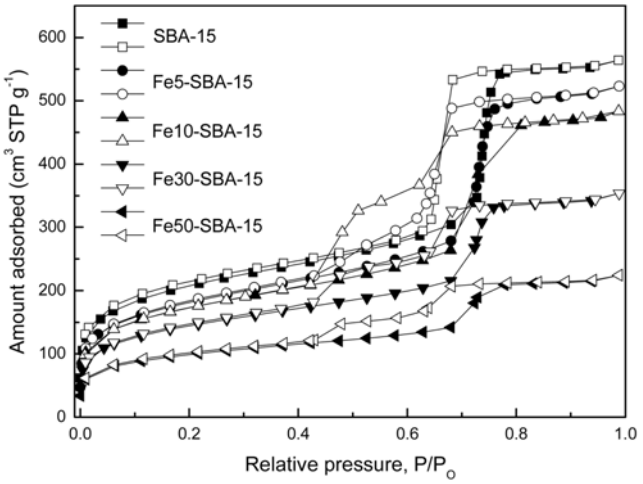

Fig. 2. N_2 gas adsorption/desorption isotherms for SBA-15 and Fe_xSBA-15. Solid and hollow symbols represent adsorption and desorption branches, respectively.

Table 1. Physical properties of the prepared Fe-impregnated mesoporous silicates

Sample	Surface area, m^2/g	Pore volume, cm^3/g	Pore size, nm BJH
SBA-15	751	0.872	5.75
Fe_5SBA-15	637.2	0.8089	5.15
Fe_{10}SBA-15	611.3	0.7475	4.37
Fe_{30}SBA-15	512.1	0.5471	4.42
Fe_{50}SBA-15	348.7	0.3470	4.47

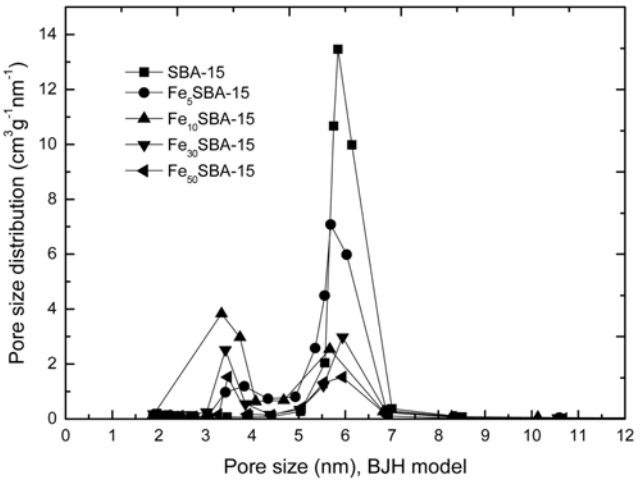

Fig. 3. Pore size distributions of SBA-15 and Fe_xSBA-15.

g with increasing amounts of added Fe. As the surface areas of Fe-impregnated SBA-15 decreased with increasing Fe amounts, so did the pore volumes of the materials; the average pore diameter D_{BJH} decreased from about 5.7 to 4.4 nm with Fe-impregnation (Table 1). Accordingly, Fe-impregnation induced a reduction in the surface area and pore diameter of the samples.

To investigate the change in pore size distribution (PSD) with

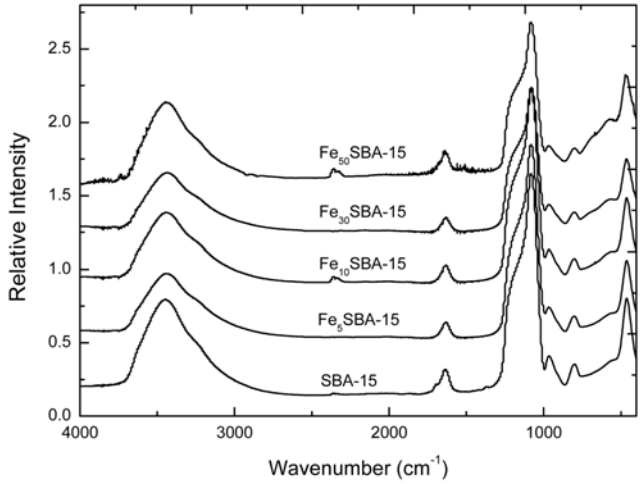

Fig. 4. FT-IR patterns of SBA-15 and Fe_xSBA-15.

Fe-impregnation, the BJH approach using nitrogen isotherms was adopted. The PSD plots were derived from the desorption branch of the nitrogen hysteresis (Fig. 3). The PSD of SBA-15 was unimodal with a sharp peak around 6 nm, whereas Fe-impregnated SBA-15 showed a bimodal distribution of pore sizes. Therefore, the reduction in the average pore sizes with Fe-impregnation was caused by the bimodal pore size distribution of Fe-impregnated SBA-15.

Fig. 4 shows the IR patterns of SBA-15 and Fe-impregnated SBA-15 between the wave numbers 400-4,000 cm^{-1}. The three peaks at 465 cm^{-1}, 800 cm^{-1}, and 1,085 cm^{-1} were assigned to rocking, bending (or symmetric stretching), and asymmetric stretching of the intertetrahedral oxygen atoms in the SiO_2 structure, respectively, for the IR patterns of SBA-15 [28]. The peak at 960 cm^{-1} corresponds to the stretching of non-bridging oxygen atoms ($Si\text{-}O^{\delta-}$) of a Si-OH stretch [28]. The peaks at 1,085 cm^{-1} and the shoulder between the IR bands of 1,100-1,300 cm^{-1} correspond to the concerted (Si-O-Si) stretches. With Fe-impregnation, the absorbance intensities of 960 cm^{-1} decreased slightly, implying that Si-OH groups interacted with Fe species. Compared to other cases [27,28], the IR peak of Si-OH at 960 cm^{-1} still remained clear, even with high Fe content. In the cases of Al and La, the impregnation of active species into SBA-15 diminished the IR band intensity of Si-OH. In contrast, the intensity of Si-OH in the IR pattern of Fe_{50}SBA-15 was still relatively high due to heterogeneous impregnation of Fe, as evidenced by the bimodal pore size distributions.

2. Adsorption Behavior of Tetracycline onto Fe-impregnated SBA-15

The adsorption kinetic data of tetracycline for the adsorbents and fitting lines from the pseudo-second-order-kinetic model are presented in Fig. 5. When the absorption ability of SBA-15 for tetracycline was evaluated, it was found to be too low to be detected. In contrast, as seen in Fig. 5, Fe-impregnated SBA-15 exhibited increased and measurable adsorption ability for tetracycline, clearly indicating that the Fe species are the adsorption sites for tetracycline. The adsorption capacity varied with the amount of Fe added. The q_e or adsorption amount of tetracycline at equilibrium was obtained by fitting the adsorption kinetic data to a pseudo second-order kinetic model and is listed in Table 2. The adsorption capacity of

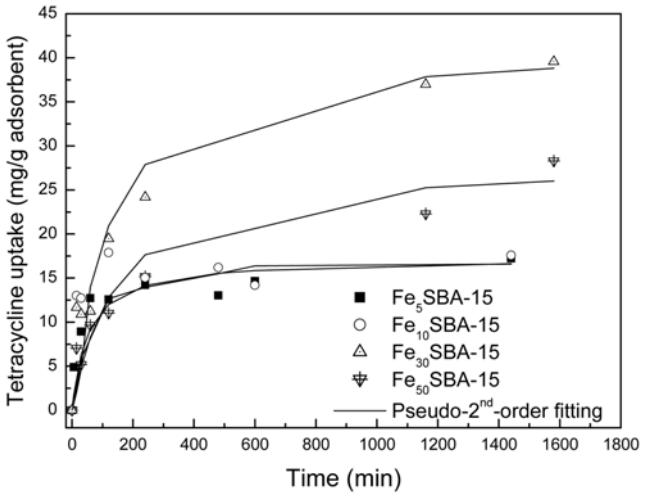

Fig. 5. Adsorption kinetic data of tetracycline for various Fe-impregnated SBA-15 samples (Solution pH=7.0, initial concentration=100 ppm).

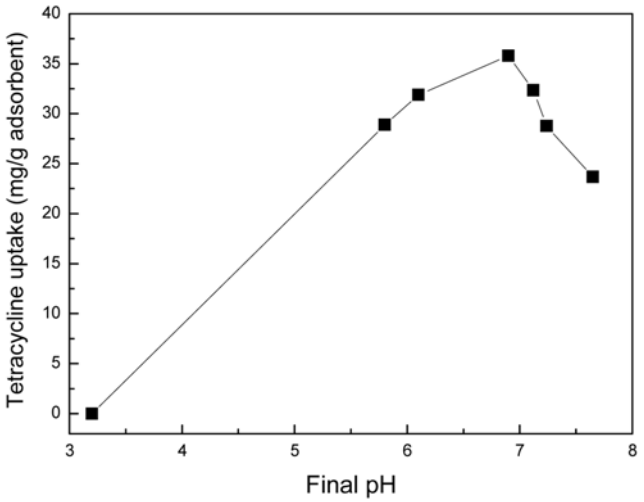

Fig. 6. Adsorption envelopes of Fe_{30}SBA-15 for tetracycline (initial concentration=100 ppm).

Table 2. The parameters acquired from the fit of adsorption kinetic data to the pseudosecond-order model

Sample	q_e, mg/g	K, g/mg·min	R^2
SBA-15	-	-	-
Fe_5SBA-15	17.2	0.00111	0.989
Fe_{10}SBA-15	17.3	0.00224	0.991
Fe_{30}SBA-15	41.7	0.00020	0.994
Fe_{50}SBA-15	28.4	0.00024	0.974

Fe_{30}SBA-15 was the highest at 41.7 mg/g. The adsorption capacity of Fe_xSBA-15 for tetracycline increased up to 30 wt% Fe loading. When Fe was loaded at 50 wt%, the tetracycline adsorption capacity decreased. This indicates that there is an optimal Fe content that is related to the dispersion of Fe species inside mesopores of SBA-15. In the adsorption of anionic pollutants onto Al impregnated SBA-15, the adsorption capacity showed a similar trend to Fe content [28]. This result suggests that dispersion of Al species and different complexation modes between anionic pollutants and adsorbents is responsible for the adsorption capacity of adsorbents. The adsorption capacity for tetracycline depends on how well the Fe species are dispersed in SBA-15 and how the Fe species interact with tetracycline. The tetracycline adsorption capacity of Fe_{30}SBA-15 in this study, 41.9 mg/g, is comparable to that observed with other adsorbents. It has been reported that the hydrous oxide of Fe adsorbs about 17.7-53.3 mg/g of tetracycline [7]. Using Na-montmorillonite, a Q_{max} (maximum adsorption capacity) of 49.3 mg/g was obtained from the fit of the Langmuir isotherm model for tetracycline adsorption [29].

Fig. 6 indicates the pH dependency of tetracycline adsorption onto Fe_{30}SBA-15. As seen there, the pattern of a pH dependency is a volcano curve; the adsorption capacity for tetracycline is the highest at neutral conditions, which is consistent with previous studies [7,14]. When ofloxacin interacted with alumina and silica, the highest adsorption capacity was found at neutral conditions [14]. The authors hypothesized that the dissociated 3-carboxyl group (COO^-) of zwitterionic ofloxacin was adsorbed on the $\equiv AlOH_2^+$ surface sites. Gu and Karthikeyan [7] studied the interaction of tetracycline with iron hydrous oxides and suggested a surface complexation mechanism. According to their suggestion, a positive surface charge such as $\equiv Fe\text{-}OH_2^{+0.5}$ interacts with negative tetracycline via the tricarbonylamide group in ring A and carbonyl group in ring C. Similarly, in this study, the positive surface charge of the Fe species in Fe-impregnated SBA-15 formed a complex through the tricarbonylamide group in ring A and the carbonyl group in ring C of tetracycline.

CONCLUSIONS

Fe-impregnated mesoporous silicates were prepared using an incipient wetness impregnation technique to facilitate adsorption of tetracycline in an aqueous system. The adsorption capacities of the Fe-impregnated mesoporous silicates for tetracycline varied according to Fe loading amounts, indicating that the dispersion of Fe species inside mesopores determines the adsorption ability of Fe-impregnated mesoporous silicates. The adsorption of tetracycline may be accomplished by the formation of surface complexes between the positive surface charges of the Fe species and the negative charges of the tricarbonylamide group in ring A and the carbonyl group in ring C of tetracycline.

ACKNOWLEDGMENTS

This work was financially supported by the Ulsan Regional Environmental Technology Development Center.

REFERENCES

1. I. Dalmázio, M. O. Almeida, R. Augusti and T. M. A. Alves, *J. Am. Soc. Mass. Spectrom.*, **18**, 679 (2007).
2. Y. Chen, C. Hu, J. Qu and M. Yang, *J. Photoch. Photobio. A*, **197**, 81 (2008).
3. M. A. Khan, J. Mustafa and J. Musarrat, *Mutat. Res. Fund. Mol. M.*, **525**, 109 (2003).

4. H. Sanderson, F. Ingerslev, R. A. Brain, B. Halling-Sørensen, J. K. Bestari, C. J. Wilson, D. J. Johnson and K. R. Solomon, *Chemosphere*, **60**, 619 (2005).
5. Y. Zuo, K. Zhang and Y. Deng, *Chemosphere*, **63**, 1583 (2006).
6. J. W. Fritz and Y. Zuo, *Food Chem*., **105**, 1297 (2007).
7. C. Gu and K. G. Karthikeyan, *Environ. Sci. Technol*., **39**, 2660 (2005).
8. C. Gu, K. G. Karthikeyan, S. D. Sibley and J. A. Pedersen, *Chemosphere*, **66**, 1494 (2007).
9. K. J. Choi, S. G. Kim and S. H. Kim, *J. Hazad. Mater*., **151**, 38 (2008).
10. S. A. Sassman and L. S. Lee, *Environ. Sci. Technol*., **39**, 7452 (2005).
11. M. Puanngam and F. Unob, *J. Hazad. Mater*., **154**, 578 (2008).
12. T. Yokoi, T. Tatsumi and H. Yoshitake, *Bull. Chem. Soc. Jpn*., **76**, 847 (2003).
13. J. C. Park, J. B. Joo and J. Yi, *Korean J. Chem. Eng*., **22**, 276 (2005).
14. K. W. Goyne, J. Chorover, J. D. Kubicki, A. R. Zimmerman and S. L. Brantley, *J. Colloid Interf. Sci.*, **283**, 160 (2005).
15. H. Yoshitake, T. Yokoi and T. Tatsumi, *Chem. Mater.*, **15**, 4536 (2003).
16. K. F. Lam, K. L. Yeung and G. McKay, *Micropor. Mesopor. Mater*., **100**, 191 (2007).
17. D. P. Quintanilla, A. Sánchez, I. Hierro, M. Fajardo and I. Sierra, *J. Colloid Interf. Sci.*, **313**, 551 (2007).
18. V. Antochshuk, O. Olkhovyk, M. Jaroniec, I. S. Park and R. Ryoo, *Langmuir*, **19**, 3031 (2008).
19. D. Li, Y. Zheng and X. Wang, *Appl. Catal. A*, **340**, 33 (2008).
20. R. A. Shaikh, G. Chandrasekar, K. Biswas, J. S. Choi, W. J. Son, S. Y. Jeong and W. S. Ahn, *Catal. Today*, **132**, 52 (2008).
21. M. R. Unnithan, V. P. Vinod and T. S. Anirudhan, *J. Appl. Polymer Sci.*, **84**, 2541 (2002).
22. E. W. Shin, J. S. Han and S. H. Min, *Environ. Technol*., **25**, 185 (2004).
23. D. E. Moore, P. Fallon and C. D. Burt, *Int. J. Pharmacol*., **14**, 133 (1983).
24. H. Oka, Y. Ikai, N. Kawamura, M. Yamada, K. Harada, S. Ito and M. Suzuki, *J. Agric. Food Chem*., **37**, 226 (1989).
25. M. M. Beliakova, S. I. Bessonov, B. M. Sergeyev, I. G. Smirnova, E. N. Dobrov and A. M. Kopylov, *Biochemistry (Mosc)*, **68**, 182 (2003).
26. X. N. Lu, J. M. Xu, W. Z. Ma and Y. F. Lu, *Pedosphere*, **17**, 124 (2007).
27. M. Jang, J. K. Park and E. W. Shin, *Micropor. Mesopor. Mater.*, **75**, 159 (2004).
28. E. W. Shin, J. S. Han, M. Jang, S. H. Min, J. K. Park and R. M. Rowell, *Environ. Sci. Technol*., **38**, 912 (2004).
29. R. A. Figueroa, A. Leonard and A. A. Mackay, *Environ. Sci. Technol*., **38**, 476 (2004).